

Stochastic Point-Source Modeling of Ground Motions in the Cascadia Region

Gail M. Atkinson

Carleton University

David M. Boore

U.S. Geological Survey

ABSTRACT

A stochastic model is used to develop preliminary ground motion relations for the Cascadia region for rock sites. The model parameters are derived from empirical analyses of seismographic data from the Cascadia region. The model is based on a Brune point-source characterized by a stress parameter of 50 bars. The model predictions are compared to ground-motion data from the Cascadia region and to data from large earthquakes in other subduction zones. The point-source simulations match the observations from moderate events ($M < 7$) in the Cascadia region. The simulations predict a steeper attenuation than observed for very large subduction events ($M \geq 7.5$) in other regions; motions are overpredicted near the earthquake source and underpredicted at large distances (>100 km). The discrepancy at large magnitudes suggests further work on modeling finite-fault effects and regional attenuation is warranted. In the meantime, the preliminary equations are satisfactory for predicting motions from events of $M < 7$ and provide conservative estimates of motions from larger events at distances less than 100 km.

INTRODUCTION

Ground-motion relations, which estimate peak ground motions or response spectral ordinates as a function of earthquake magnitude and distance, are a critical component of seismic hazard analysis. In eastern North America (ENA), ground-motion relations have been developed using a stochastic point-source model, with model parameters selected based on analysis of regional seismographic data and strong-motion data (see papers in this volume by Atkinson and Boore and Toro *et al.*). These relations were based on a research effort spanning more than a decade. In the Cascadia region of western Washington and southwestern British Columbia, by contrast, there has been relatively little research aimed at the development of regional ground motion relations, despite a growing recognition of the earthquake hazard. It has generally been assumed that the ground motions for crustal earthquakes in the Cascadia region will

be adequately predicted using empirical relationships developed for California. For deeper earthquakes associated with subduction, empirical relationships developed using data from other subduction zones are assumed (*e.g.*, Youngs *et al.*, 1988; Crouse, 1991; Geomatrix, 1993).

A recent study of the source characteristics and attenuation of ground motions in the Cascadia region (Atkinson, 1995) indicates that the direct application of California ground-motion relations is not readily justified. Moderate Cascadia earthquakes are characterized by lower stress drop (*i.e.*, lower near-source high-frequency amplitudes) than are California earthquakes of similar size, and the motions attenuate more slowly with distance. Furthermore, crustal earthquakes in Cascadia occur over a much wider range in focal depth. We therefore require ground-motion relations that are specific to the Cascadia subduction region. The applicability of ground-motion relations based on data from other subduction zones (*e.g.*, Youngs *et al.*, 1988; Crouse, 1991; Geomatrix, 1993) cannot be directly assessed, since there are no data from great earthquakes in the Cascadia subduction zone.

In this paper, we develop preliminary ground-motion relations for Cascadia based on a stochastic point-source model, with model parameters chosen based on regional seismographic data. Simulations are made for a range of moment magnitudes (M , Hanks and Kanamori, 1979) from 4 to 8.25 at hypocentral distances (r_{hypo}) from 10 to 400 km. Being based on a point-source model, the ground-motion relations are not expected to be valid for large earthquakes ($M > 7$). We compare these preliminary relations with data from large subduction earthquakes in other regions to judge the need for modifications to the methodology to account for finite-fault effects. The point-source relations are also compared with data from moderate events in the Cascadia region.

GROUND-MOTION SIMULATIONS FOR CASCADIA

Ground motions for earthquakes in the Cascadia region are simulated using the stochastic point-source method (Hanks and McGuire, 1981; Boore, 1983; Boore and Atkinson, 1987; Atkinson and Boore, 1995 and this volume). The

method and computer codes are fully described in Boore (1996) and summarized in our ENA paper in this volume. Seismographic data from the Cascadia region (Atkinson, 1995, 1996a) were used to define the elements required to describe the model for the earthquake spectrum as a function of moment magnitude (M), hypocentral distance (r_{hypo}) and frequency (f):

$$E(M, r_{\text{hypo}}, f) = E(M, f) D(r_{\text{hypo}}, f) S(f) P(f) I(f) \quad (1)$$

$E(M, f)$ is the earthquake source spectrum (*i.e.*, Fourier spectrum of the ground acceleration at a distance of 1 km). Based on analysis of seismographic data for Cascadia events from M 3.7 to 6.7, we adopt a Brune (1970, 1971) source model with a stress parameter of 50 bars (Atkinson, 1995; also Figure 8). The crustal properties used with the Brune model are 2.8 gm/cm^3 for density and 3.7 km/sec for shear-wave velocity in the source region; an average radiation pattern of 0.55 was assumed, with a factor of $1/\sqrt{2}$ for vectorial partition into two horizontal components, and a factor of 2 for free-surface amplification.

$D(r_{\text{hypo}}, f)$ is a diminution function that models the geometric and anelastic attenuation of the spectrum. It is defined here by r_{hypo}^{-1} geometric spreading, and anelastic attenuation is given by $Q = 380f^{0.39}$. This is a simplification of the empirically-observed attenuation, which is depth-dependent (Atkinson, 1995, 1996b). Shallow events ($h < 20$ km) attenuate more steeply than this initially, then more slowly in the distance range from 75 to 230 km, probably due to strong reflected phases from mid-crustal discontinuities, the Moho, and the subducting slab. Deep events follow the simple R^{-1} attenuation curve over all distances. The simplification introduced here is justified by the preliminary nature of the relations and the relatively low engineering significance of the differences in attenuation shape at $R > 100$ km.

$S(f)$ is a site amplification factor for "typical" rock sites in the Cascadia region. The simplified crustal profiles of Tohee *et al.* (1991) indicate that the near-surface rock has near-wave velocities that increase from about 1.5 km/sec at the surface to 3.7 km/sec at a few km depth. Based on the quarter-wavelength approximation of Joyner and Fumal (1985), this would produce a ground-motion amplification with a weak frequency-dependence (factor of 1.45 at 0.5 Hz, increasing to 1.55 at 10 Hz); we therefore assume a simple amplification factor $S(f)=1.5$ for all frequencies.

$P(f)$ is a high-cut filter that reduces amplitudes at high frequencies ($f > 5$ Hz); for Cascadia we use the kappa model (Anderson and Hough, 1984) with a value of $k_0=0.011$ for average rock sites (Atkinson, 1996a).

$I(f)$ is a filter used to shape the spectrum to correspond to the particular ground motion measure of interest. For example, for the computation of response spectra, I is the response of an oscillator to ground acceleration.

The final input element of the stochastic predictions is the duration of motion. The duration model has two terms:

$$T = T_o + T_d \quad 2$$

where T_o is the source duration and T_d represents a distance-dependent term which accounts for dispersion. For the source duration, we assume that $T_o = 1/f_o$, where f_o is the corner frequency of the Brune source spectrum (Brune, 1970). The distance-duration term is based on empirical data for the region (Atkinson, 1995):

$$T_d = 0 \quad r_{\text{hypo}} \leq 50 \text{ km} \quad (3a)$$

$$T_d = 0.07 (r_{\text{hypo}} - 50) \quad r_{\text{hypo}} > 50 \text{ km} \quad (3b)$$

Using the inputs described above, response spectra (5% damped pseudo-absolute acceleration, SA) for frequencies of 0.5 Hz to 20 Hz, and peak ground acceleration (PGA) and velocity (PGV) were simulated for $4.0 \leq M \leq 8.25$ in 0.25 magnitude-unit increments from $r_{\text{hypo}} = 10$ km to $r_{\text{hypo}} = 400$ km. Fifty trials were used for each magnitude-distance combination. The results provide median ground motions, under the point-source assumption, for the random horizontal component at rock sites ($\beta = 1.5$ to 2 km/sec).

Quadratic-Equation Form of Ground Motion Simulations

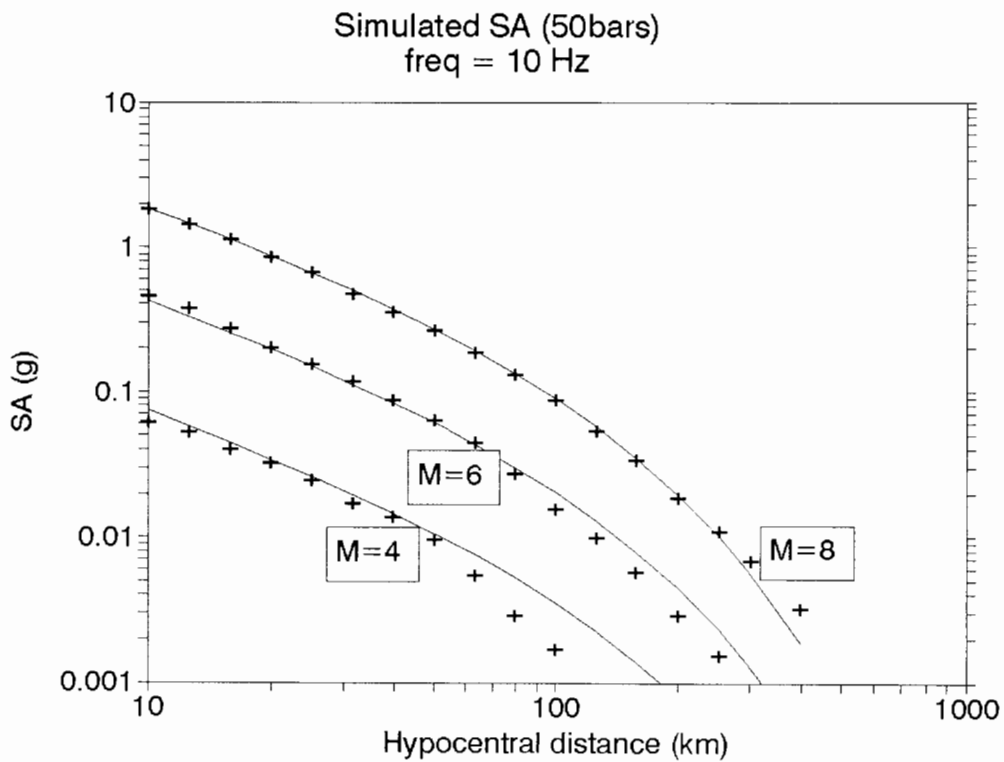
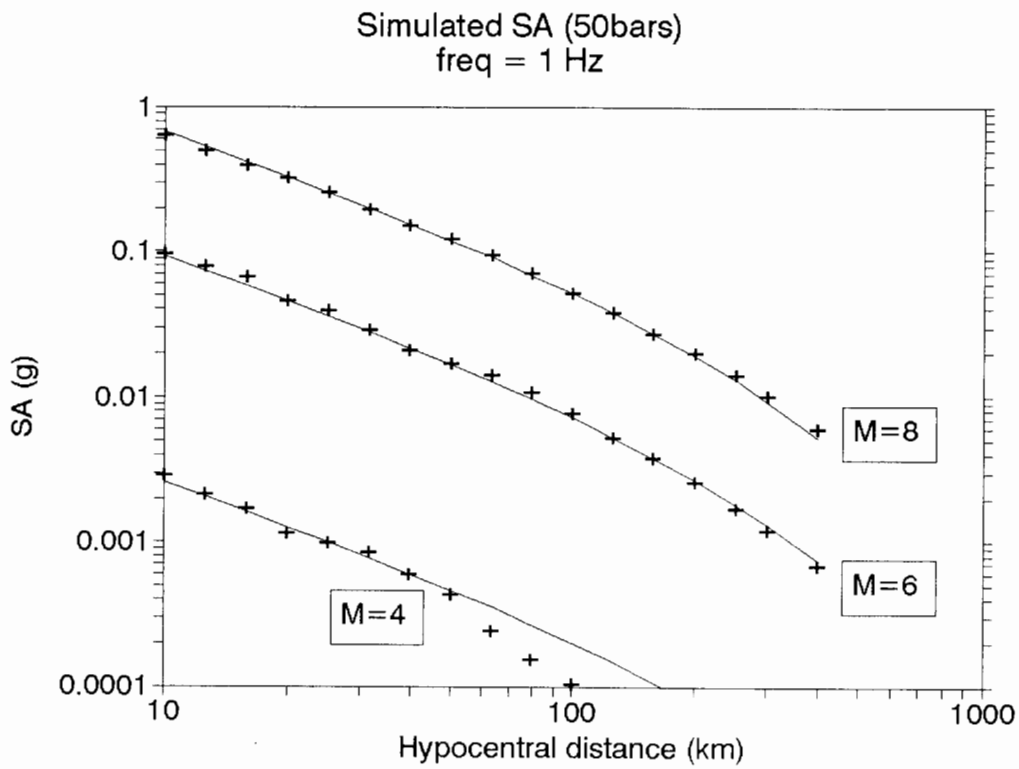
Figure 1 plots the attenuation of the simulated SA values for frequencies of 1 and 10 Hz (symbols). The figure also shows simple quadratic equations that approximate the estimates for the purposes of seismic hazard calculations. The coefficients of the quadratic equations are listed in Table 1.

The quadratic equations were obtained by regression of a subset of the simulated ground motion data. The subset included the simulated values from all distances ($r_{\text{hypo}} \leq 400$ km) for large events ($M \geq 6$) but only near distances ($r_{\text{hypo}} \leq 35$ km) for small events ($4 \leq M < 6$). This constrains the attenuation to match the relatively slow decay of motions that is applicable for the larger earthquakes. In Figure 1 it is clear that the quadratic equations track the simulated amplitudes closely, with the exception of the values for small events at distances greater than 30 km. This exception was deliberate. The objective was to fit the magnitude-dependent shape of the results with a simple functional form that is convenient to use in hazard analyses and is sufficiently accurate in the magnitude-distance ranges that are significant to seismic hazard analysis.

COMPARISON OF PRELIMINARY GROUND MOTION MODEL WITH DATA

Ground Motion Database

The validity of the point-source ground motion simulations can be judged by comparing the model predictions to ground motion data. For these comparisons, the ground motion database is comprised of response spectra computed from moderate earthquakes recorded on the Western Canada Telemetered Network (WCTN) (rock sites), as well as



▲ **Figure 1.** Predicted response spectral values (SA for 5% damping) for frequencies of 1 and 10 Hz, for $M=4$, 6 and 8. Symbols represent ground motion predictions. Lines show quadratic equations of Table 1.

SA, PGA in g, PGV in cm/s $\ln SA = c_1 + c_2(M-6) + c_3(M-6)^2 - \ln r_{\text{hypo}} - c_4 r_{\text{hypo}}$				
Frequency (Hz)	c_1	c_2	c_3	c_4
0.5	-0.912	1.565	-0.172	0.00207
0.8	-0.295	1.457	-0.201	0.00276
1.0	-0.033	1.388	-0.201	0.00299
1.3	0.232	1.322	-0.195	0.00345
2.0	0.650	1.174	-0.165	0.00414
3.2	1.001	1.041	-0.117	0.00530
5.0	1.273	0.929	-0.076	0.00645
8.0	1.472	0.851	-0.044	0.00783
10.0	1.530	0.809	-0.032	0.00829
20.0	1.470	0.733	0.000	0.00921
PGA	0.680	0.733	0.000	0.00645
PGV	4.903	1.223	0.000	0.00253

strong-motion data from Puget Sound (soil), Japan (soil), Mexico (rock and soil), Chile (rock and soil) and Alaska (rock). The Cascadia region data are from Atkinson (1995); data from other subduction zones are from Crouse (1990). Only events recorded on at least three stations are included, to minimize bias. Figure 2 summarizes the database for the comparisons. Note that the recordings for moderate events come almost entirely from the Cascadia region, while those for large events come entirely from other subduction zones; there are no data in the magnitude range from M 6.8 to M 7.4. The focal depth of the events ranges from 1 to 60 km.

Correction of Soil Records to Reference Rock

The database contains a mixture of rock and soil recordings. Although velocity profiles are not available for the soil sites, it is believed that the sites classified as firm soil by Crouse (1991) correspond, approximately, to Boore *et al.*'s (1993) Class C site conditions (Crouse, personal communication, 1995). These sites have an average shear-wave velocity of 255 m/s in the upper 30 m. The few soft soil records in the database are assumed to correspond to Boore *et al.*'s (1993) Class D, with average $\beta = 125$ m/s. Rock sites are assumed to have an average β of approximately 1,500 to 2,500 m/s, based on the simplified crustal profiles of Cohee *et al.* (1991).

In order to compare the data with the predicted ground motion amplitudes for rock, all soil recordings were "corrected" to equivalent rock amplitudes by dividing the SA values by factors given in Table 2 (from Atkinson, 1996b). These factors were based on the empirical analysis results of Boore *et al.* (1994), utilized to convert amplitudes from the specified average β values to Boore *et al.*'s (1993) reference velocities for California rock, V_A ; a small additional correc-

freq(Hz)	BV	VA	a_1	a_2	Factor ($a_1 * a_2$)
0.5	-0.655	1790	3.58	1.06	3.79
0.6	-0.697	1520	3.47	1.15	3.98
1.0	-0.698	1410	3.30	1.19	3.93
1.3	-0.666	1480	3.23	1.16	3.75
1.6	-0.622	1590	3.12	1.12	3.50
2.0	-0.553	1780	2.93	1.06	3.10
2.5	-0.487	1950	2.69	1.01	2.73
3.1	-0.420	2100	2.42	0.98	2.37
4.0	-0.360	2170	2.16	0.96	2.08
5.0	-0.292	2120	1.86	0.97	1.80
7.9	-0.221	1600	1.50	1.12	1.68
10.0	-0.212	1110	1.37	1.34	1.83

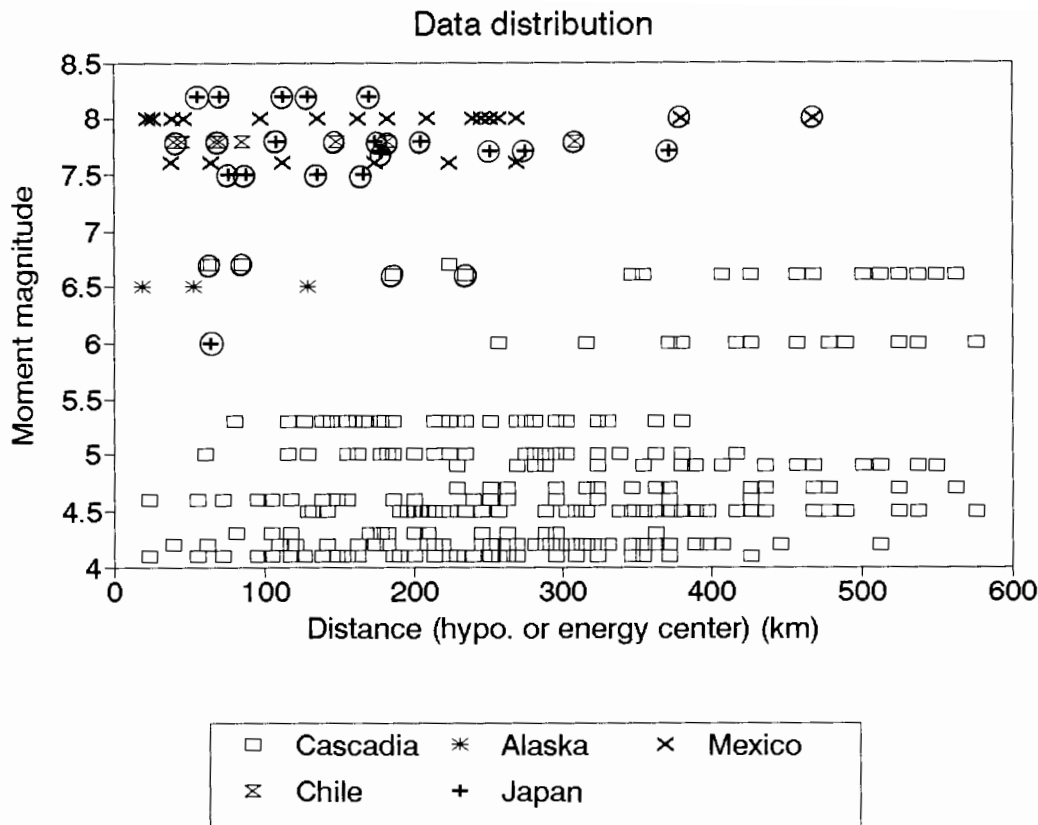
Notes: BV and VA are from Boore *et al.* (1994)
 $a_1 = 10^{[BV(\log \beta - \log VA)]}$ for $\beta = 255$ m/s
 $a_2 = \sqrt{\frac{2000}{VA}}$

tion factor based on impedance contrast then converts from the V_A values to an average "hard rock" velocity of 2 km/sec. As described in our ENA paper (this volume), this correction is subject to considerable uncertainty, perhaps as much as a factor of 1.5 to 2; there are other possible approximations that would appear to be equally valid. The data comparisons should be viewed with caution in light of this uncertainty.

H/V Correction for Vertical Records

The strong-motion data from other subduction regions include two horizontal components of ground motion, both of which are used in the comparisons. The WCTN instruments record only the vertical component, and these data are converted to an equivalent single horizontal component. The ratio of the random horizontal component to the vertical component (H/V) is generally considered to be a stable site characteristic, depending on the velocity profile of the site (Gupta *et al.*, 1989; Theodulidis *et al.*, 1996); in fact, a common method of measuring the shear-wave velocity profile (referred to as Nakamura's technique) is based on this ratio. With the possible exception of recordings very near the earthquake source ($R < 20$ km), H/V is independent of earthquake magnitude and distance (Atkinson, 1993) and independent of source location or mechanism (Theodulidis *et al.*, 1996). Thus a reliable estimate of the horizontal-component motion can be obtained from the vertical-component data if the shear-wave velocity profile of the recording site is known.

The velocity profiles of the WCTN sites are not known. The recent M 5.1 Duvall, Washington earthquake of



▲ Figure 2. Summary of SA data for comparison with predictions, by magnitude and distance. Circled points are soil recordings; all others are rock.

the 05/03 and its many aftershocks provided an opportunity to measure the H/V ratio, as several hard rock sites in the region have been instrumented with three-component broadband seismometers within the past few years. The H/V ratio is similar for each of the three rock sites for which a good set of records is available, although the event-to-event and site-to-site variability is significant. Figure 3 plots the average value of $\log H/V$, and the standard deviation of the measurements, as obtained from a total of 50 records (Duvall events of $M \geq 3.0$ plus a $M 2.0$ earthquake near Victoria, B.C.). The average H/V is larger at high frequencies than the ratio obtained by Atkinson (1993) for eastern hard rock sites; this suggests that WCTN sites have lower near-surface velocities than ECTN sites. Based on the new H/V data, the smooth solid curve on Figure 3 was adopted for use in estimating the average horizontal component from the vertical-component WCTN data in the frequency range from 0.5 to 10 Hz. This function is given by:

$$\log H/V = 0.07 + 0.25 \log f \quad (4)$$

with the constraint $0 \leq \log H/V \leq 0.25$. Considering uncertainty in both the H/V and soil factor corrections, the "data" to be compared with the predictions for rock sites in Cascadia should be considered uncertain by as much as a factor of two.

Comparisons of Data with Simulations

The database, corrected to represent the horizontal component of rock motion as described above, is compared to the simulations through plots of residuals; the residual is defined as the natural log of the observed PSA value minus the natural log of the predicted value. In Figure 4, we examine the residuals as a function of distance for just the subset of data from the Cascadia region (depth > 2 km). The residuals do not show any clear trends with distance, and any effects of focal depth on the pattern of residuals appear to be minor. Residuals for a group of four events of $M 3.7$ to $M 4.6$, tightly clustered in both time and space, were eliminated from these plots; the events occurred at very shallow depth (1 to 2 km) and had very low Brune stress parameters (10 bars) relative to other shallow crustal events at $h > 2$ km (and thus very low ground motion amplitudes). Inclusion of the events would suggest a greater depth effect on the residuals than that indicated in Figure 4; however, we believe that this effect is probably not representative of shallow events in general (such as the Duvall event at $h = 7$ km, which had a much larger stress parameter; see also Figure 8).

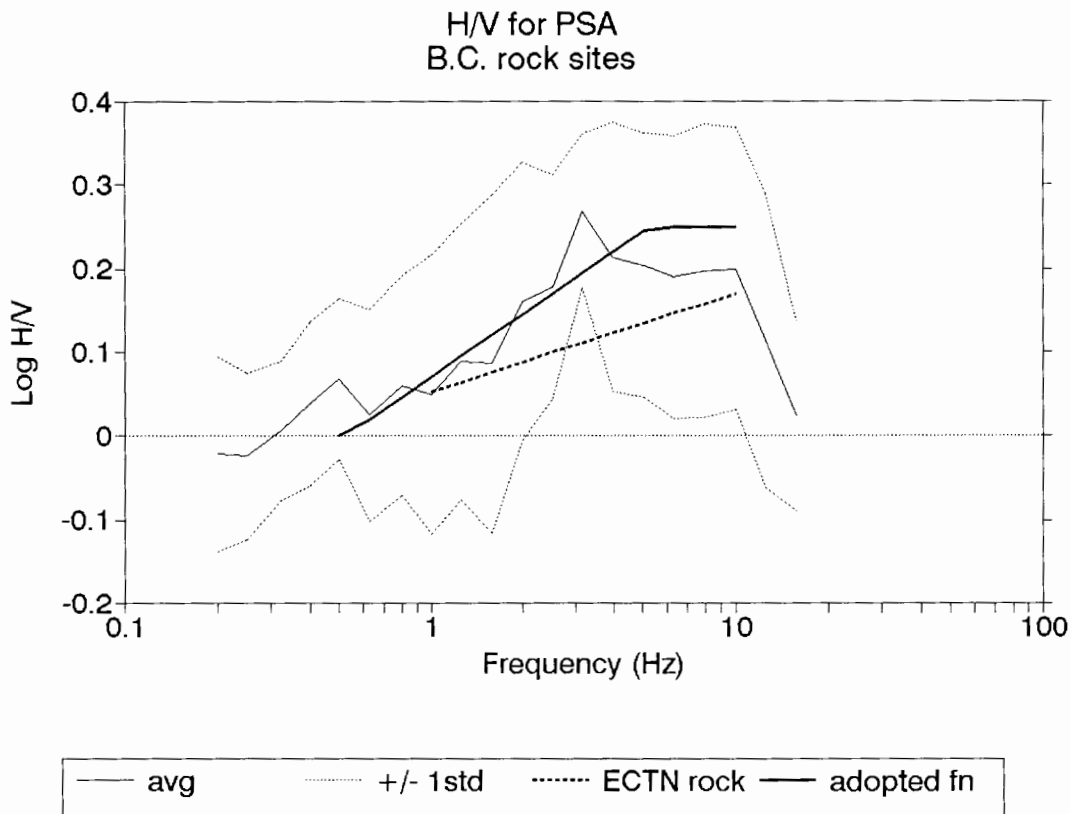
The average residual for just the Cascadia data is 0.00 for all frequencies from 1 to 10 Hz (the range of the data); the standard deviation of residuals is large, increasing with frequency from a value of 0.55 ln units at 1 Hz to 0.78 ln units at 10 Hz. The increase in variability with frequency

▲ Figure 3
Plots show
Observation
Canada Tel

may be an
the WCTN

In Fig
other subd
the region
significant tr
relations. Inc
the del. prec
km. u
uncles. H
eg. ins are
of data
total for
 ≤ 5 Hz
The am
deases fr
in variab
tion of ve

Figure 7
are not
of that d
variable
of 0.55



▲ **Figure 3.** Horizontal-to-vertical component ratio at rock sites in British Columbia. Light solid line shows mean H/V at B.C. sites; dotted lines show standard deviation of measurements. Heavy solid line is H/V function adopted in this study to convert vertical component observations to equivalent horizontal component. Heavy dashed line shows average H/V ratio for rock sites as recorded on the Eastern Canada Telemetered Network.

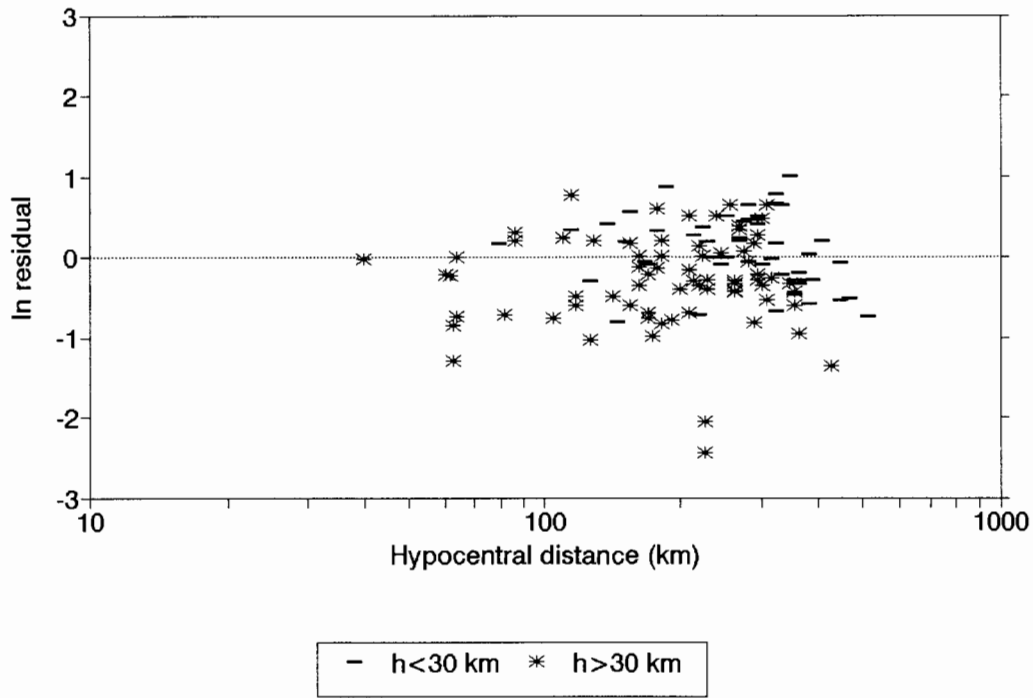
may be an indication of high-frequency rock site effects in the WCTN data.

In Figure 5, the distance-dependence of the residuals for other subduction regions is compared to that for the Cascadia-region data. At low frequencies ($f < 5$ Hz) there is a significant trend in the residuals for the data from other regions, indicating lesser attenuation than that used in the model predictions (overprediction of amplitudes at $r_{hypo} < 100$ km, underprediction at $r_{hypo} > 100$ km). At high frequencies ($f > 5$ Hz), the residuals for the data from other regions are consistently low (overprediction), with the exception of data in the 60–120 km distance range. The average residual for the data from other subduction regions is 0.00 for $f \leq 5$ Hz, then decreases to a value of -0.37 ln units for 10 Hz amplitudes; the standard deviation of residuals decreases from 0.81 ln units at 1 Hz to 0.62 at 10 Hz. The large variability at low frequencies may be reflecting the effects of variability in soil conditions of the recording sites.

Figure 6 plots the residuals as a function of magnitude. There are no obvious trends. Overall, it appears from Figures 4 to 6 that the 50-bar point-source stochastic simulations do a reasonable job of matching the ground-motion observations for moderate events in the Cascadia region.

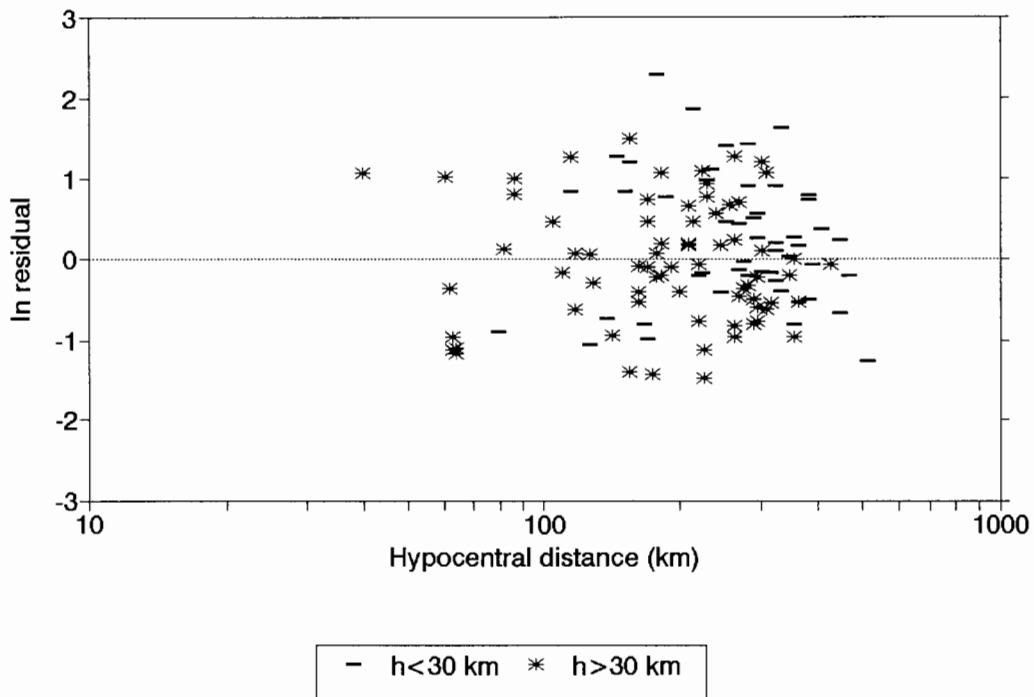
The attenuation of large ($M > 7$) subduction earthquakes in other regions appears to be significantly different than predicted by this model. This is explored further on Figure 7, which compares the predictions of the simulation model (Table 1 equations) with strictly-empirical regression equations developed by Atkinson (1996b) for the same database (*i.e.*, data of Figure 2). The empirical regression indicated a dependence of both the slope and the level of the curves on focal depth, so the empirical equations are shown for two focal depths, 10 and 50 km. The empirical regression also indicated that the attenuation rate is slower than R^{-1} for events of $M \geq 7.5$, while being consistent with R^{-1} for $4 \leq M < 7.5$; accordingly, the slope of the empirical regression curve is shallow ($R^{-0.5}$) for $M \geq 7.5$. Figure 7 suggests that the stochastic point-source model predictions are very similar to the empirical regression results for moderate events (generally M 5 to 6.5) at distances less than 200 km. The discrepancy at small magnitudes (M 4) is, for large distances, attributable to the overestimation of simulated amplitudes from small events at large distance—an artifact of the quadratic regression equations that approximate the simulations (see Figure 1). The persistence of this discrepancy at close distances

SA residuals (50 bar simulations)
Cascadia data: freq = 1 Hz



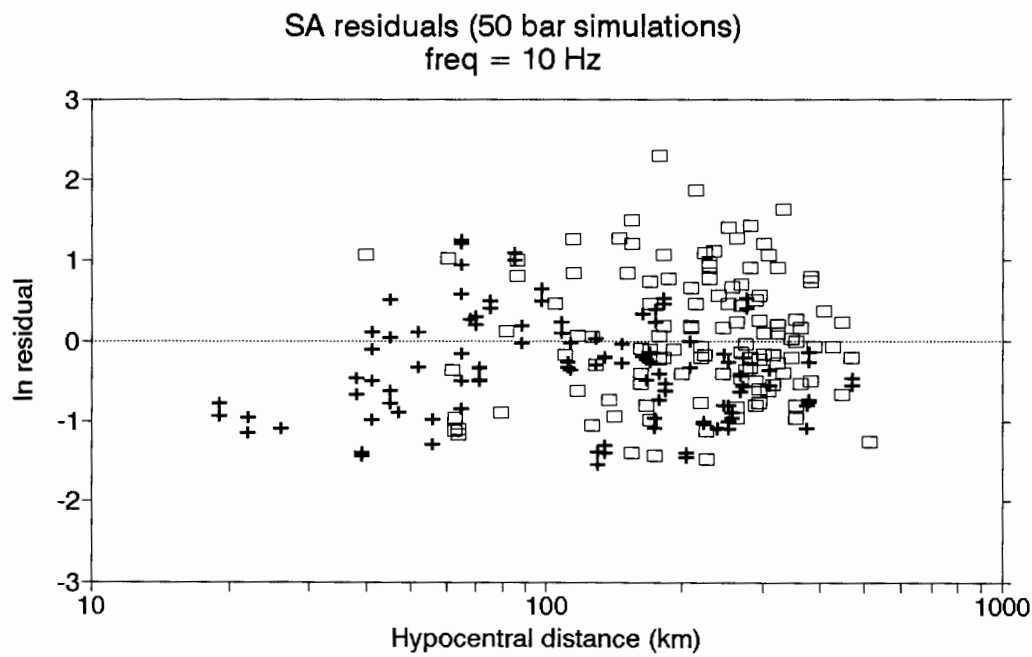
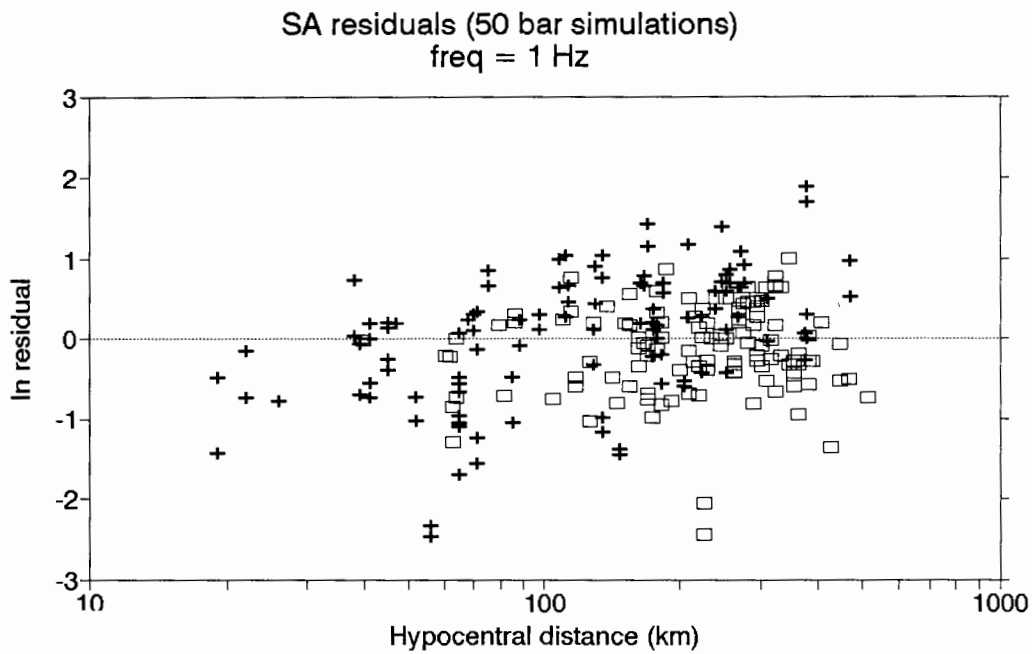
(a)

SA residuals (50 bar simulations)
Cascadia data: freq = 10 Hz



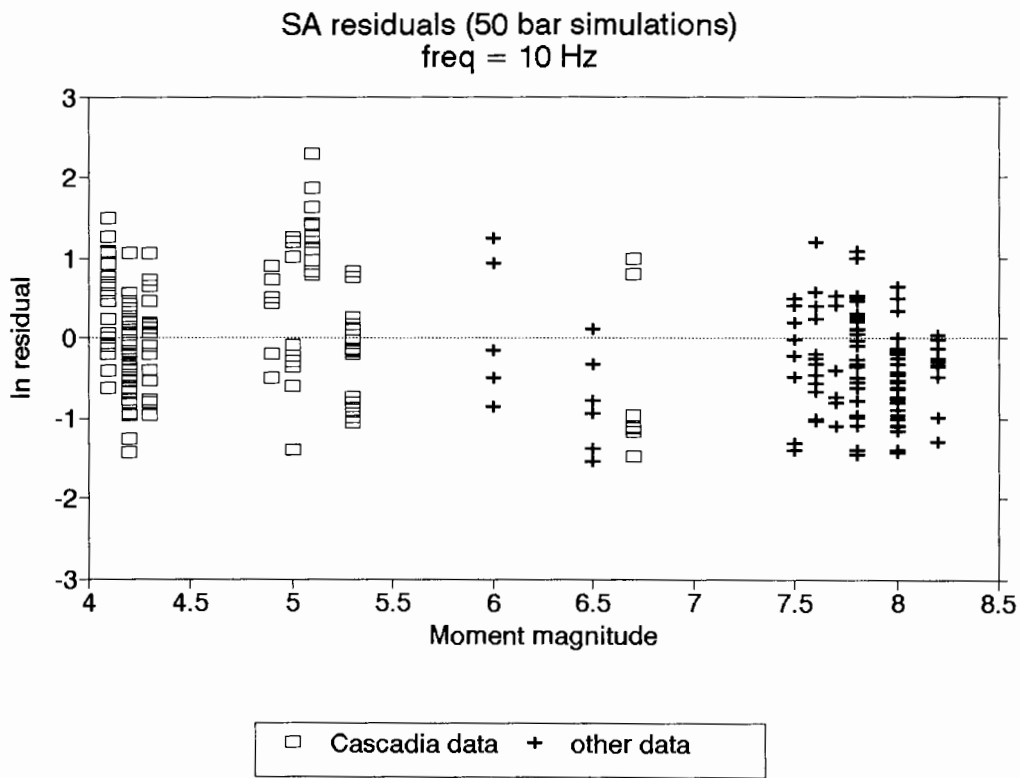
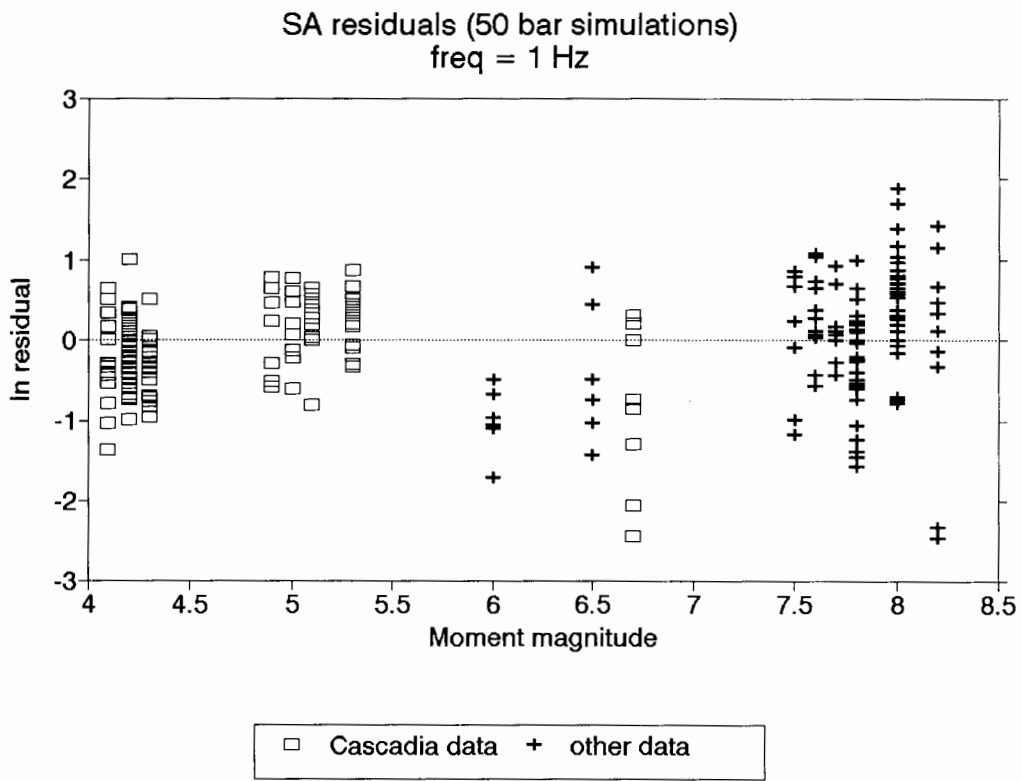
(b)

▲ Figure 4. Observed SA values for Cascadia data, minus model predictions (ln units), as a function of distance, for frequencies of 1 and 10 Hz. Events are differentiated according to focal depth (bars for $h < 30$ km, asterisks for $h > 30$ km).

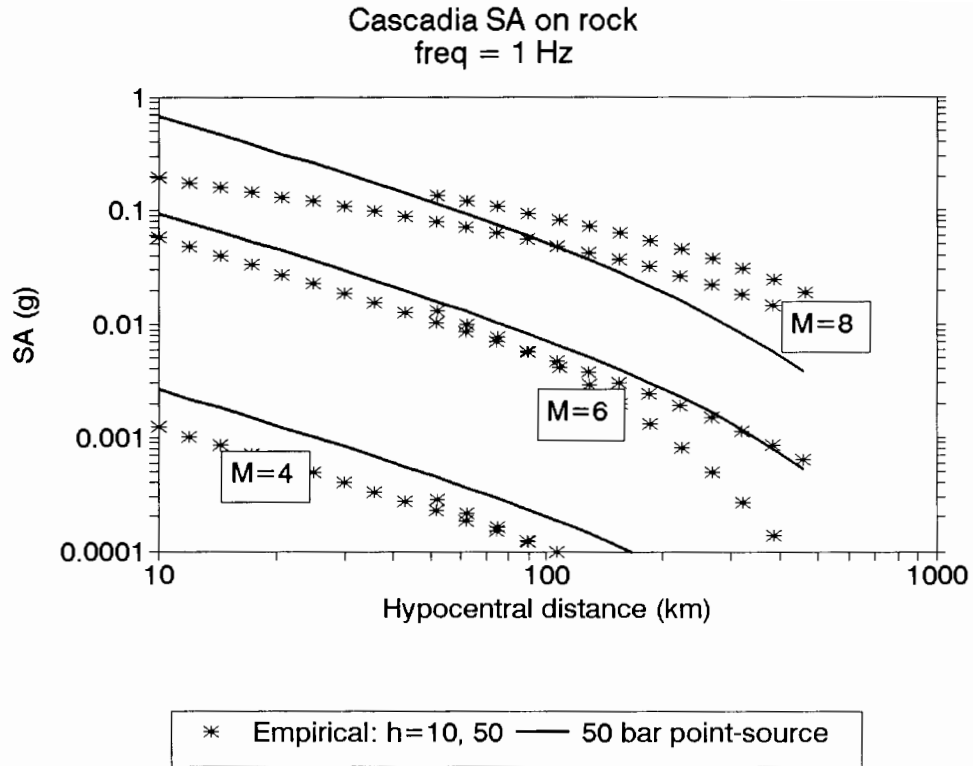


□ Cascadia data + other data

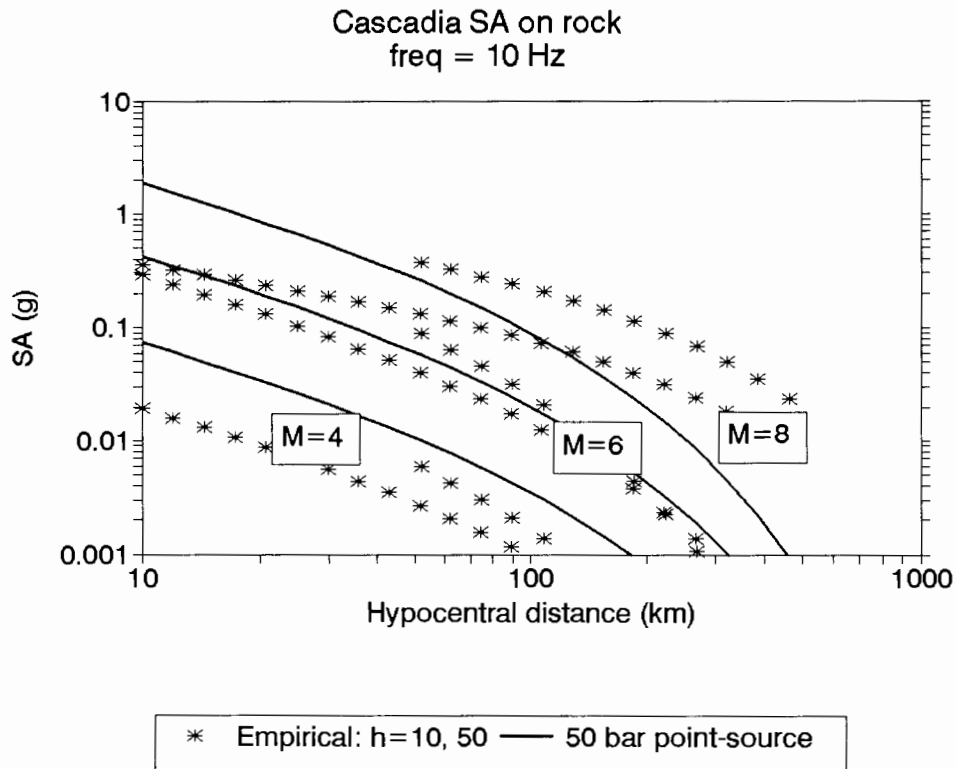
▲ **Figure 5.** Observed SA values for Cascadia data (open squares) and data from other subduction zones (plus symbols), minus model predictions (ln units), as a function of distance, for frequencies of 1 and 10 Hz.



▲ **Figure 6.** Observed SA values for Cascadia data (open squares) and data from other subduction zones (plus symbols), minus model predictions (ln units), as a function of magnitude, for frequencies of 1 and 10 Hz.

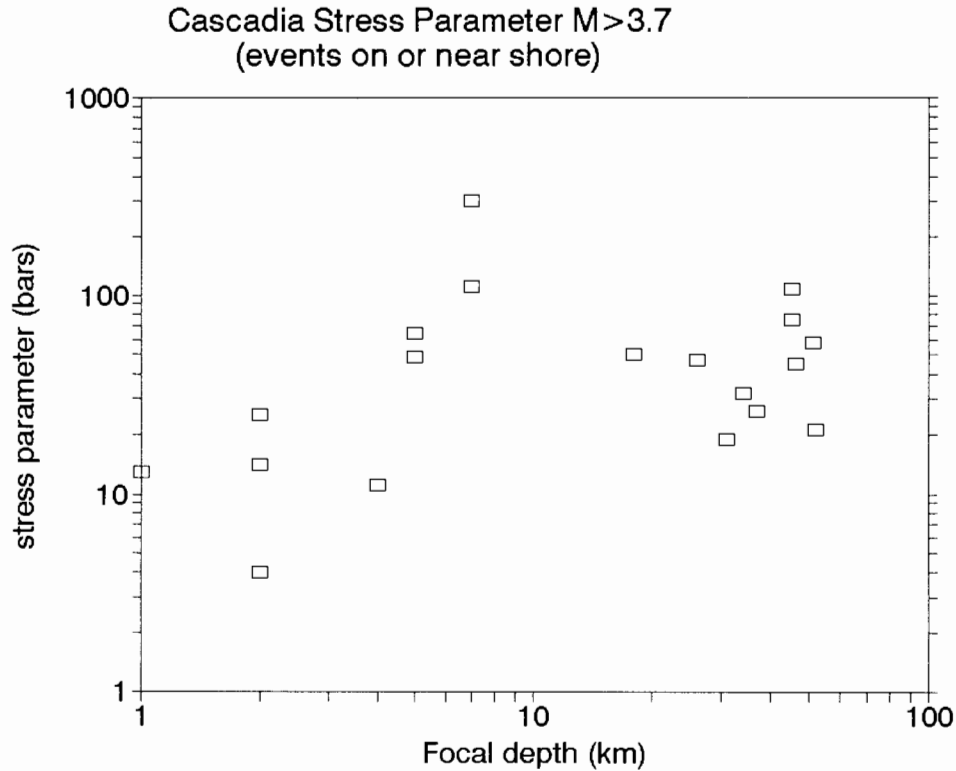


(a)



(b)

▲ **Figure 7.** Comparison of 50-bar stochastic model equations (solid lines, independent of focal depth) with predictions of the empirical regression of Atkinson, 1996b (asterisks) for events of focal depth 10 and 50 km, for frequencies of 1 and 10 Hz.



▲ **Figure 8.** Stress parameter required to match the high-frequency level of the Fourier spectrum for earthquakes in the Cascadia region as a function of focal depth for events of $M \geq 3.7$ (stress values from Atkinson, 1995).

could be a consequence of unmodeled magnitude dependence of attenuation in the empirical model.

There are two major discrepancies between the predictions and the empirical regressions that are as yet unresolved. First, it is clear that the attenuation of the large subduction events from other regions is slower than that predicted by the simulations. This is probably a finite-fault effect. The distance measure used in the Crouse (1991) dataset is the closest distance to the center of energy release, which would correspond to the distance to the equivalent point source. Within a broad zone above an extended fault source, however, we may draw increasingly nearer to this point while seeing about the same strength of radiation emanating from the fault plane. If the discrepancy in attenuation rates is indeed a finite-fault effect, it suggests that the simulation model should be modified for large magnitude events to account for such effects. On the other hand, it is possible that the discrepancy in apparent attenuation is due to other factors. These other possibilities include unmodeled site effects or regional differences in attenuation, possibly due to features such as a velocity inversion in the crust (recall that all of the large events are from other regions). To explore these possibilities adequately, further work is needed to model the fault geometry and ground motion observations from the large events in more detail.

The second discrepancy that must be resolved concerns the dependence of the attenuation and the level of the curves on focal depth. Such effects are clearly indicated by empirical regression of the combined dataset, but careful examination of just the Cascadia data makes these effects appear unconvincing. For example, as shown on Figure 8, an apparent trend of Brune stress parameter with focal depth disappears if the four tightly-clustered events at $h < 3$ km, as discussed earlier, are discounted (this leaves just one low-stress event at $h = 4$ km). The dependence of attenuation rate on depth is more clear-cut but does not appear to significantly affect the residuals for the Cascadia region (see Figure 4), and thus may be neglected for engineering applications.

In summary, the stochastic model predictions for a Brune point-source model with a stress parameter of 50 bars match data from the Cascadia region for events of moderate magnitude ($M < 7$). There are significant discrepancies between the model attenuation and that observed in the data from very large subduction events ($M \geq 7.5$) recorded in other regions. Further work is required to determine the cause of these discrepancies and improve the model accordingly; finite-fault effects are a likely explanation, but other possibilities cannot be discounted. In the meantime, the preliminary equations given in Table 1 provide satisfactory ground motion estimates for moderate ($M < 7$) Cascadia earthquakes in the focal depth range from 5 to 60 km and

conservative estimates of motions for events of $M > 7$ at distances less than 100 km. ☒

ACKNOWLEDGMENTS

C. B. Crouse generously shared his database. Maureen Dowd (U.S.G.S.) digitized the tables provided by C.B. Crouse. We thank Tom Hanks and Harley Benz for their reviews. This work was funded by the National Earthquake Hazards Reduction Program (Grant 1434-95-G-2522).

REFERENCES

- Anderson, J. and S. Hough (1984). A model for the shape of the Fourier amplitude spectrum of acceleration at high frequencies, *Bull. Seism. Soc. Am.*, **74**, 1,969–1,993.
- Anderson, G. (1993). Notes on ground motion parameters for eastern North America: Duration and H/V ratio, *Bull. Seism. Soc. Am.*, **83**, 587–596.
- Anderson, G. (1995). Attenuation and source parameters of earthquakes in the Cascadia region, *Bull. Seism. Soc. Am.*, **85**, 1,327–1,342.
- Anderson, G. (1996a). The high-frequency shape of the source spectrum for earthquakes in eastern and western Canada, *Bull. Seism. Soc. Am.*, **86**, 106–112.
- Anderson, G. (1996b). Empirical ground motion relations for earthquakes in the Cascadia region, *Can. J. Civil Eng.*, submitted.
- Anderson, G. and D. Boore (1995). New ground motion relations for eastern North America, *Bull. Seism. Soc. Am.*, **85**, 17–30.
- Boore, D. (1983). Stochastic simulation of high-frequency ground motions based on seismological models of the radiated spectra, *Bull. Seism. Soc. Am.*, **73**, 1,865–1,894.
- Boore, D. (1996). SMSIM—Fortran programs for simulating ground motions from earthquakes, Version 1.0. *U.S. Geol. Surv. Open-file Report 96-80-A*.
- Boore, D. and G. Atkinson (1987). Stochastic prediction of ground motion and spectral response parameters at hard-rock sites in eastern North America, *Bull. Seism. Soc. Am.*, **77**, 440–467.
- Boore, D., W. Joyner, and T. Fumal (1993). Estimation of response spectra and peak accelerations from western North American earthquakes: An interim report, *U.S. Geological Survey Open-file 93-509*.
- Boore, D., W. Joyner, and T. Fumal (1994). Estimation of response spectra and peak accelerations from western North American earthquakes: An interim report, Part 2, *U.S. Geological Survey Open-file 94-127*.
- Brune, J. (1970). Tectonic stress and the spectra of seismic shear waves from earthquakes, *J. Geophys. Res.*, **75**, 4,997–5,009.
- Brune, J. (1971). Correction, *J. Geophys. Res.*, **76**, 5002.
- Cohee, B., P. Somerville, and N. Abrahamson (1991). Simulated ground motions for hypothesized $M_w = 8$ subduction earthquakes in Washington and Oregon, *Bull. Seism. Soc. Am.*, **81**, 28–56.
- Crouse, C. (1990). *Ground-motion attenuation equations for Cascadia subduction zone earthquakes*, Report to the U.S. Geological Survey and Electric Power Research Institute.
- Crouse, C. (1991). Ground-motion attenuation equations for Cascadia subduction zone earthquakes, *Earthquake Spectra*, **7**, 201–236.
- Geomatrix (1993). Seismic margin earthquake for the Trojan site: Final unpublished report prepared for Portland General Electric Trojan Nuclear Plant, Ranier, Oregon.
- Gupta, I., K. McLaughlin, R. Wagner, R. Jih, and T. McElfresh (1989). *Seismic wave attenuation in eastern North America*, Report NP-6304, Electric Power Research Institute, Palo Alto, Calif.
- Hanks, T., and H. Kanamori (1979). A moment magnitude scale, *J. Geophys. Res.*, **84**, 2,348–2,350.
- Hanks, T. and R. McGuire (1981). The character of high-frequency strong ground motion, *Bull. Seism. Soc. Am.*, **71**, 2,071–2,095.
- Joyner, W. and T. Fumal (1985). Predictive mapping of ground motion, in Ziony (ed.), *Evaluating earthquake hazards in the Los Angeles Region*, *U.S. Geol. Surv. Prof. Paper 1360*, 203–220.
- Theodulidis, N., P. Bard, R. Archuleta, and M. Bouchon (1996). Horizontal-to vertical spectral ratio and geological conditions: The case of Garner Valley downhole array in southern California, *Bull. Seism. Soc. Am.*, **86**, 306–319.
- Youngs, R., S. Day, and J. Stevens (1988). Near field ground motions on rock for large subduction earthquakes, *Proceedings of the 2nd Conference on Earthquake Engineering and Soil Dynamics*, Geotechnical Division ASCE, Park City, Utah, 27–30 June 1988, 445–462.

Department of Earth Sciences
Carleton University
Ottawa, Ont. K1S 5B6
(613) 623-3240 (phone and FAX)
email: gma@ccs.carleton.ca
(G.M.A.)

U.S. Geological Survey
345 Middlefield Rd.
Menlo Park, Ca. 94025
(415) 329-5616
email: boore@samoa.wr.usgs.gov
(D.M.B.)